Influence of Specific Interactions on the Rotational Dynamics of Charged and Neutral Solutes in Ionic Liquids Containing Tris(pentafluoroethyl)trifluorophosphate (FAP) Anion

ARTICLE *in* THE JOURNAL OF PHYSICAL CHEMISTRY B · JULY 2010

Impact Factor: 3.3 · DOI: 10.1021/jp1039282 · Source: PubMed

1 AUTHOR:

GB Dutt
Bhabha Atomic Research Centre
75 PUBLICATIONS **1,636** CITATIONS

SEE PROFILE

Influence of Specific Interactions on the Rotational Dynamics of Charged and Neutral Solutes in Ionic Liquids Containing Tris(pentafluoroethyl)trifluorophosphate (FAP) Anion

G. B. Dutt*

Radiation & Photochemistry Division, Bhabha Atomic Research Centre, Trombay, Mumbai 400 085, India

Received: April 30, 2010; Revised Manuscript Received: June 3, 2010

Rotational dynamics of two organic solutes, rhodamine 110 (R110) and 2,5-dimethyl-1,4-dioxo-3,6-diphenylpyrrolo[3,4-*c*]pyrrole (DMDPP), has been investigated as a function of temperature in a series of 1-alkyl-3-methylimidazolium ionic liquids (alkyl = ethyl, butyl, hexyl, and 2-hydroxyethyl) containing tris(pentafluoroethyl)trifluorophosphate (FAP) anion. The present study has been essentially undertaken to examine the influence of specific interactions on the rotation of cationic (R110) and neutral (DMDPP) solutes in this new class of ionic liquids. Analysis of the results using the Stokes−Einstein−Debye hydrodynamic theory indicates that the rotational dynamics of R110 is closer to the stick boundary condition whereas the dynamics of DMDPP is described by the slip boundary condition. The observed slow dynamics of R110 has been rationalized on the basis of specific interactions between the cationic solute and the FAP anion of the ionic liquid. It has also been noticed that the rotational dynamics of DMDPP is slower by 30% in 1-(2-hydroxyethyl)-3-methylimidazolium FAP compared to that observed in its ethyl counterpart, which is assimilated in terms of hydrogen bonding interactions between the carbonyl groups of the solute and the hydroxyl group of the imidazolium cation.

1. Introduction

Investigations dealing with rotational dynamics of organic solutes in ionic liquids can be used to explore the interactions that prevail between the solute and the constituent cations and anions of the ionic liquid. Understanding these interactions is essential to exploit the tremendous potential of these ionic liquids in catalysis, synthesis, and solvent extraction.[1−5] Since the first study by Bright and co-workers[6] in 2001, quite a few studies have appeared in literature dealing with the rotational dynamics of neat ionic liquids[7] and organic solutes dissolved in ionic liquids.[8−18] As a result, a wealth of information has been generated pertinent to solute−solvent interactions in these systems. Maroncelli and co-workers[8−11] have found that the rotational correlation functions of solutes in ionic liquids are usually described by stretched-exponential functions of time unlike in low viscosity conventional solvents. This kind of behavior has been attributed to non-Markovian friction effects, which are more evident in ionic liquids because of their higher viscosities. Except for this unusual behavior, solute rotation in ionic liquids and conventional solvents are almost similar. Castner and co-workers,[12] on the other hand, have observed multiexponential rotational correlation functions of solutes in ionic liquids. The fast time constants have been attributed to the solute molecule experiencing microviscosity that is orders of magnitude below the measured shear viscosities, whereas the slow time constants provide the evidence for either complex nanostructural reorganization or embedding of the solute in rather large ion clusters. Recent results from our group[13,14] suggest that specific interactions between the solute molecules and the anions of the ionic liquids are imperative to explain the solute rotation in ionic liquids, while the results of Paul and Samanta[15] and Fruchey and Fayer[16] establish the role of specific interactions between the solute and the cation of the ionic liquid in describing the solute rotation.

In most of these studies,[6,8−18] alkyl substituted imidazolium, pyrrolidinium, ammonium and phosphonium derivatives have been used as cations in conjunction with anions such as hexafluorophosphate, tertafluoroborate, bromide, chloride, dicyanamide, ethylsulfate, bis(trifluoromethylsulfonyl)imide and tris(trifluoromethylsulfonyl)methide. It must be noted that, barring a few studies,[10,14,16] a majority of the investigations have been carried out with neutral solutes in ionic liquids as quite a few charged solutes are not soluble in the highly charged ionic liquid environments. In view of the paucity of experimental data, the influence of ion−ion interactions between the charged solutes and ionic liquids on solute rotational dynamics is not clearly understood. Thus, the present study has been undertaken, wherein rotational dynamics of cationic and neutral solutes has been examined in a new class of ionic liquids containing tris(pentafluoroethyl)trifluorophosphate (FAP) anion.

The synthesis of ionic liquids containing FAP anion was reported by Ignat'ev and co-workers[19] in 2005. Although developed as replacements for ionic liquids containing hexafluorophosphate anion, this group of ionic liquids possess interesting properties such as excellent hydrolytic, thermal and electrochemical stability.[20] Moreover, ionic liquids containing FAP anion provide numerous advantages in organic synthesis,[21] electrosynthesis,[22] gas absorption[23] and battery applications.[24,25] It has been shown that these ionic liquids are the most hydrophobic and the water uptake is much less compared to the ionic liquids containing bis(trifluoromethylsulfonyl)imide anion and it is about 10 times lower than that of ionic liquids with hexafluorophosphate anion.[20] In addition to the above-mentioned properties, the FAP anion is weakly coordinating, and hence these ionic liquids have comparatively lower viscosities. Ionic liquids containing FAP anion possess lower hydrogen bond basicity compared to tertafluoroborate, bis(trifluoromethylsulfonyl)imide, hexafluorophosphate-based ionic liquids hav-

* To whom correspondence should be addressed. E-mail: gbdutt@barc.gov.in

10.1021/jp1039282
Published on Web 06/22/2010

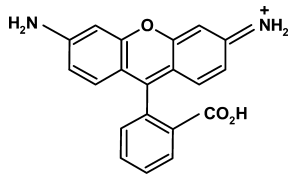

Rhodamine 110

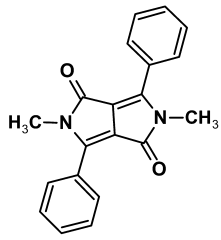

DMDPP

Figure 1. Molecular structures of the solutes used in the study.

ing the same cationic component.[26,27] In the case of hydroxyl-functionalized cations, the presence of FAP leads to an enhancement of the hydrogen bond acidity, relative to the bis(trifluoromethylsulfonyl)imide analogs. Despite the existence of numerous studies,[5,19−27] which unravel various physicochemical properties of the ionic liquids containing FAP anion, to the best of our knowledge no dynamical studies have been reported in these systems up until now and the work described here is a small step in that direction.

In this work, time-resolved fluorescence anisotropy measurements of two organic solutes, rhodamine 110 (R110) and 2,5-dimethyl-1,4-dioxo-3,6-diphenylpyrrolo[3,4-*c*]pyrrole (DMDPP), have been carried out in 1-ethyl-3-methylimidazolium FAP ([EMIM][FAP]), 1-butyl-3-methylimidazolium FAP ([BMIM][FAP]), 1-hexyl-3-methylimidazolium FAP ([HMIM][FAP]) and 1-(2-hydroxyethyl)-3-methylimidazolium FAP ([HEMIM][FAP]) over the temperature range 298−348 K. Figure 1 gives the molecular structures of the solutes used in the study. The objective of this work is to explore how the hydrogen bond accepting ability of the FAP anion and hydrogen bond donating capacity of hydroxyl-functionalized imidazolium cation influence the rotational dynamics of charged and neutral solutes. The other motive is to examine the role of the alkyl chain length of the imidazolium cation on solute rotation.

2. Experimental Section

The four ionic liquids containing the FAP anion used in this study were purchased from Merck, Germany. The purity of the liquids is >99% with <100 ppm water content and <100 ppm halide ion concentration. The probes R110 and DMDPP were obtained from Exciton and Ciba Specialty Chemicals, Inc., respectively. All of these chemicals are of the highest available purity and were used without further purification. Concentrations of the probes in the ionic liquids were chosen such that at the wavelength of excitation, which is 445 nm for both R110 and DMDPP, the absorbance is less than 0.2.

Time-resolved fluorescence measurements were carried out with a setup that works on the principle of time-correlated single-photon counting.[28] The setup used in the present study was purchased from IBH, U.K. and employs a diode laser as the excitation source. Samples containing the probes R110 and DMDPP in ionic liquids were excited with a 445 nm diode laser whose pulse width is <100 ps and repetition rate is 1 MHz. Fluorescence signal from the sample was detected at right angles to the excitation source with the help of a monochromator and a Peltier cooled microchannel plate detector. The emission from the samples was monitored at 550 nm. Since the repetition rate of the laser is 1 MHz, the decays were acquired by operating the time-to-amplitude converter in the inverted mode to avoid pulse pile-up distortions. The decays were collected in 4096 channels with a time increment of 14.4 ps/channel. The instrument response function (IRF) of the setup was measured by collecting the scattered light from a TiO_2 suspension in water, and the full-width at half-maximum (FWHM) was found to be around 100 ps. For lifetime measurements, decays were collected by keeping the emission polarizer at magic angle (54.7°) with respect to the polarization of the excitation laser to ensure the complete depolarization of the fluorescence. Anisotropy decay measurements were carried out by collecting parallel and perpendicular decay components with respect to the polarization of the excitation laser. The two decay components were acquired for at least 900 s each such that a good signal-to-noise ratio was obtained. To account for the discrepancies in transmission efficiency of the monochromator, the perpendicular component was corrected for the G-factor of the spectrometer. The measurements were carried over the temperature range 298−348 K, and the temperature of the sample was controlled with the aid of a thermoelectric controller (model DS) from IBH. Each measurement was repeated 2−3 times, and the average values are reported. The analyses of fluorescence and anisotropy decays were performed using the software supplied by IBH. The anisotropy decays were analyzed using the impulse reconvolution method as well as tail fit of the anisotropy data (without reconvolution). Both of the methods of analysis yielded identical numbers for the anisotropy decay constants since the smallest time constant measured in the present study is 450 ps, which is 4 times longer than the FWHM of the IRF. The viscosities of the four ionic liquids were measured as a function of temperature using a Physica MCR 101 rheometer.

3. Results and Discussion

The anisotropy decays, $r(t)$ of both R110 and DMDPP in the four ionic liquids could be adequately fitted with a single exponential function over the temperature range 298−348 K and the functional form is given below.

$$r(t) = r_0 \exp(-t/\tau_r) \quad (1)$$

In the above equation, r_0 is the limiting anisotropy and τ_r is the reorientation time. Anisotropy decays of R110 and DMDPP in the four ionic liquids at 298 and 348 K are displayed in Figures 2 and 3, respectively. It can be noticed from the figures that the anisotropy decays become progressively slower from [EMIM][FAP] to [HEMIM][FAP] due to an increase in the viscosities of the ionic liquids. The reorientation times of R110 and DMDPP in the four ionic liquids as a function of temperature along with the solvent viscosities are listed in Tables 1 and 2, respectively. The uncertainties on τ_r values are usually in the range of 5−10%, except for R110 in [HEMIM][FAP] at 298 K, where the error is about 15% because the recovered reorientation time is 4 times longer than the fluorescence lifetime. The uncertainties on the measured viscosities (η) are about 5%. Figure 4 gives plots of $\log(\eta)$ versus $1/T$ for the four ionic liquids and it can be noticed from the figure that there is a gradual increase in the viscosity with an increase in the alkyl chain length on the imidazolium cation. However, the viscosities of [HEMIM][FAP] are higher by a factor of 3.4−1.6 compared

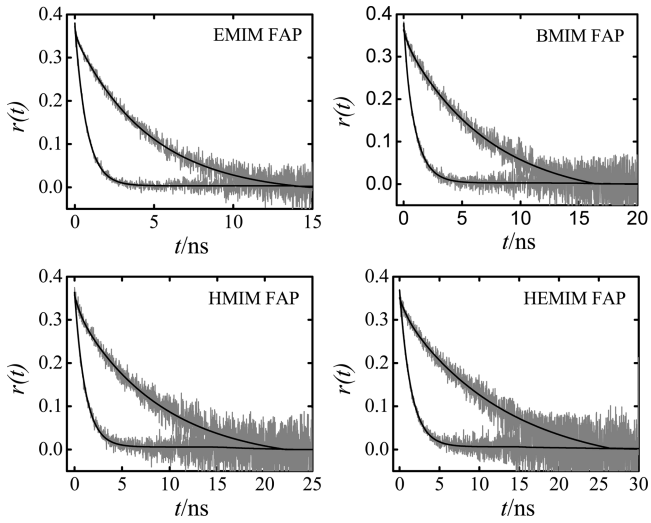

Figure 2. Anisotropy decays of R110 in the four ionic liquids at 298 and 348 K. The smooth lines passing through the experimental curves are the fitted ones. Notice that the anisotropy decays become progressively slower from [EMIM][FAP] to [HEMIM][FAP] due to an increase in the viscosities of the ionic liquids.

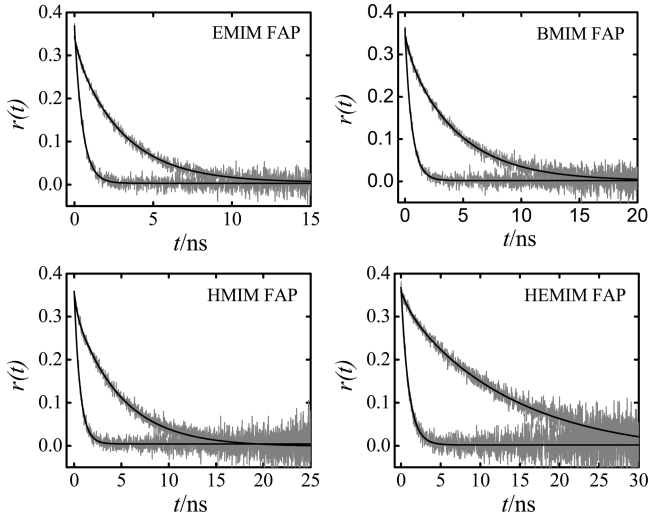

Figure 3. Anisotropy decays of DMDPP in the four ionic liquids at 298 and 348 K. The smooth lines passing through the experimental curves are the fitted ones. Notice that the anisotropy decays become progressively slower from [EMIM][FAP] to [HEMIM][FAP] due to an increase in the viscosities of the ionic liquids.

TABLE 1: Reorientation Times of R110 in the Four Ionic Liquids as a Function of Temperature Along with their Viscosities

	[EMIM][FAP]		[BMIM][FAP]		[HMIM][FAP]		[HEMIM][FAP]	
T/K	η/mPa s	τ_r/ns	η/mPa s	τ_r/ns	η/mPa s	τ_r/ns	η/mPa s	τ_r/ns
298	60.0	4.88	75.1	7.25	89.6	8.84	205.0	16.0
303	50.0	4.05	60.0	5.87	72.0	7.01	147.0	11.2
308	42.0	3.21	49.2	4.74	58.0	5.79	111.0	8.60
313	35.0	2.59	40.8	3.84	47.1	4.61	86.0	6.60
318	29.7	2.05	33.8	3.12	38.6	3.69	67.3	5.31
323	25.2	1.71	28.6	2.50	32.1	3.02	53.5	4.20
328	21.8	1.38	24.2	2.05	27.2	2.49	42.9	3.25
338	16.7	0.99	18.4	1.37	20.2	1.61	29.7	2.21
348	13.1	0.72	14.0	0.98	15.5	1.17	21.6	1.46

to [EMIM][FAP] due to the highly associative nature of the hydroxyl group.

The experimentally measured reorientation times of R110 and DMDPP have been analyzed within the framework of Stokes−Einstein−Debye (SED) hydrodynamic theory. According to this theory, the rotational diffusion of a medium sized solute molecule in a solvent continuum is assumed to occur by small-step diffusion and its reorientation time is related to the macroscopic viscosity of the solvent by the following relation.[29−31]

TABLE 2: Reorientation Times of DMDPP in the Four Ionic Liquids as a Function of Temperature Along with their Viscosities

	[EMIM][FAP]		[BMIM][FAP]		[HMIM][FAP]		[HEMIM][FAP]	
T/K	η/mPa s	τ_r/ns	η/mPa s	τ_r/ns	η/mPa s	τ_r/ns	η/mPa s	τ_r/ns
298	60.0	3.12	75.1	4.39	89.6	4.99	205.0	13.6
303	50.0	2.47	60.0	3.51	72.0	3.79	147.0	9.45
308	42.0	1.93	49.2	2.62	58.0	3.03	111.0	6.52
313	35.0	1.61	40.8	2.17	47.1	2.33	86.0	4.69
318	29.7	1.24	33.8	1.77	38.6	1.78	67.3	3.53
323	25.2	1.01	28.6	1.36	32.1	1.49	53.5	2.84
328	21.8	0.85	24.2	1.10	27.2	1.19	42.9	2.20
338	16.7	0.62	18.4	0.75	20.2	0.84	29.7	1.35
348	13.1	0.45	14.0	0.56	15.5	0.61	21.6	0.92

$$\tau_r = \frac{\eta VfC}{kT} \tag{2}$$

In the above equation, k and T are Boltzmann constant and absolute temperature, respectively. V is the molecular volume and, for the purpose of calculating the reorientation time using the SED equation, the van der Waals volume of the solute is usually employed. C is the boundary condition parameter, which signifies the extent of coupling between the solute and the solvent. The two limiting cases are, the hydrodynamic stick and slip.[32] For a nonspherical solute molecule, the value of C follows the inequality, $0 < C \leq 1$ and the exact value of C is determined by the axial ratio. f is the shape factor introduced to account for the nonspherical shapes of the solute molecules.[33] The shapes of the solute molecules are usually incorporated into the SED model by treating them as either symmetric or asymmetric ellipsoids. For nonspherical molecules, $f > 1$ and the magnitude of the deviation from unity in the value of f describes the degree of nonspherical nature of the solute molecule.

The details concerning the calculation of reorientation times of R110 and DMDPP using the SED theory with slip and stick boundary conditions were described in our earlier publications.[14,34] However, salient features are mentioned here for the sake of continuity. The axial radii of both R110 and DMDPP were estimated using Corey-Pauling-Koltum scaled atomic models and are given in Table 3. The table also gives van der Waals volumes of the two solutes, which were obtained using the Edward's increment method.[35] The solute molecules were treated as asymmetric ellipsoids since the dimensions along the three

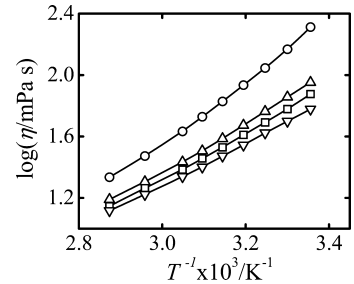

Figure 4. Plots of log (η) versus 1/T for [EMIM][FAP] (∇), [BMIM][FAP] (□), [HMIM][FAP] (Δ) and [HEMIM][FAP] (○). The lines passing through the data points are drawn as a visual aid.

TABLE 3: Solute Dimensions and van der Waals Volumes together with Shape Factors and Boundary Condition Parameters Calculated Using the SED Hydrodynamic Theory

solute	axial radii/Å^3	V/Å^3	f	C_{slip}
R110	6.7 × 5.5 × 1.8	275	2.02	0.15
DMDPP	8.2 × 4.3 × 1.9	281	2.03	0.32

axes are different. The friction coefficients with stick boundary condition along the three axes were obtained by interpolating the numerical tabulations of Small and Isenberg,[36] while the friction coefficients with slip boundary condition were obtained from the numerical tabulations of Sension and Hochstrasser.[37] From the calculated friction coefficients ζ_is along the three principal axes of rotation, the diffusion coefficients D_is were obtained using the Einstein relation.[38]

$$D_i = \frac{kT}{\zeta_i} \tag{3}$$

The reorientation time was calculated from the D_is with the aid of the following equation.[39,40]

$$\tau_r = \frac{6}{5r_0}\left[\frac{\cos^2\theta \sin^2\theta}{3(D + D_3)} + \frac{F + G}{4(6D - 2\Delta)} + \frac{F - G}{4(6D + 2\Delta)}\right] \tag{4}$$

Equation 4 can be used for calculating the reorientation time of an asymmetric rotor when the decay of anisotropy is described by a single-exponential function. Moreover, this equation is derived under the assumption that the transition dipole is in the plane of the molecule and θ is the angle between the transition dipole and the long axis of the molecule with

$$D = (D_1 + D_2 + D_3)/3 \tag{5}$$

D, the mean diffusion coefficient, is the average of the diffusion coefficients along the long axis D_1, short-in-plane axis D_2, and out-of-plane axis D_3 and

$$\Delta = (D_1^2 + D_2^2 + D_3^2 - D_1D_2 - D_2D_3 - D_3D_1)^{1/2} \tag{6}$$

$$F = \alpha_1^4 + \alpha_2^4 + \alpha_3^4 - \frac{1}{3} \tag{7}$$

$$G\Delta = D_1(\alpha_1^4 + 2\alpha_2^2\alpha_3^2) + D_2(\alpha_2^4 + 2\alpha_3^2\alpha_1^2) + D_3(\alpha_3^4 + 2\alpha_1^2\alpha_2^2) - D \tag{8}$$

In eq 8, α_is are the direction cosines of the transition moment with respect to the principal axes of rotation.[29] From the calculated τ_r values with the stick boundary condition, the shape factors were obtained using eq 2 since the value of C_{stick} is unity. The boundary condition parameter with slip boundary condition C_{slip} was obtained by taking the ratio $\tau_r^{slip}/\tau_r^{stick}$. The values of f and C_{slip} for R110 and DMDPP are also given in Table 3. Figure 5 gives plots of experimentally measured reorientation times as a function of η/T for the two solutes in the four ionic liquids and it is evident from the figure that the variation of τ_r with

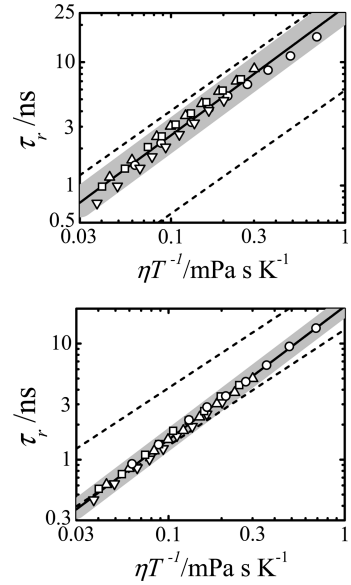

Figure 5. Plots of τ_r versus η/T for R110 (top) and DMDPP (bottom) in [EMIM][FAP] (∇), [BMIM][FAP] (□), [HMIM][FAP] (Δ) and [HEMIM][FAP] (○). The lines passing through the points were obtained by performing least-squares fit of all the data points. The shaded areas are used to highlight the data points. Theoretically calculated reorientation times using SED theory with slip and stick boundary conditions are also shown (dashed lines) in the figures.

η/T is linear for both the solutes. Theoretically calculated slip and stick lines are also shown in the figures. A quick glance at the figure reveals that the rotational dynamics of the charged solute, R110 is close to the stick hydrodynamics while the rotation of neutral solute DMDPP follows the trend predicted by the slip hydrodynamics. Essentially, two distinct sets of data points have been obtained; one corresponding to the rotation of R110 and the other corresponding to DMDPP in the four ionic liquids. The following relationships were obtained between τ_r and η/T for R110 and DMDPP from the least-squares analysis of the log−log plots.

R110

$$\tau_r = (28.1 \pm 1.9)(\eta/T)^{1.04\pm0.03}\ (N = 36, R = 0.985)$$

DMDPP

$$\tau_r = (20.9 \pm 0.7)(\eta/T)^{1.15\pm0.01}\ (N = 36, R = 0.997)$$

In these expressions, N and R are the number of data points and regression coefficient, respectively. It can be noticed from these expressions that in case of R110, the relationship between τ_r and η/T is almost linear and for DMDPP there is a slight degree of nonlinearity. To get a better appreciation of how the solute−solvent interactions vary with temperature and choice of the ionic liquid, observed boundary condition parameters C_{obs} were calculated from the experimentally measured reorientation times using the following equation, which was obtained by rearranging eq 2.

$$C_{obs} = \frac{\tau_r kT}{\eta V f} \tag{9}$$

It has been noticed that the with the exception of R110 in [HEMIM][FAP], C_{obs} decreases by 10−30% upon increasing

TABLE 4: Boundary Condition Parameters of R110 and DMDPP in the Four Ionic Liquids Obtained from the Measured Reorientation Times[a]

	C_{obs}	
ionic liquid	R110	DMDPP
[EMIM][FAP]	0.55 ± 0.05	0.33 ± 0.03
[BMIM][FAP]	0.70 ± 0.05	0.38 ± 0.03
[HMIM][FAP]	0.73 ± 0.04	0.36 ± 0.02
[HEMIM][FAP]	0.60 ± 0.02	0.42 ± 0.04
All Four Ionic Liquids	0.64 ± 0.08	0.37 ± 0.05

[a] Average boundary condition parameters obtained for R110 and DMDPP in all of the four ionic liquids are also given.

the temperature from 298 to 348 K. The probable reason for a change in the hydrodynamic boundary condition could be that the attractive solute−solvent interactions become less important at elevated temperatures.[41] The observed boundary condition parameters obtained in this manner for both the solutes in the four ionic liquids are given in Table 4. The C_{obs} value reported in the table for each solute-ionic liquid system is an average of the boundary condition parameters obtained at 9 different temperatures. The important point that needs to be emphasized from this analysis is the significant differences in the C_{obs} values of the two solutes in the four ionic liquids. The boundary condition parameter of R110 is larger compared to that of DMDPP by 67% in [EMIM][FAP] and this number increases to 84 and 103% in [BMIM][FAP] and [HMIM][FAP], respectively. In contrast, the C_{obs} values of the two solutes differ by only 43% in [HEMIM][FAP]. Moreover, C_{obs} increases by 33% for R110 from [EMIM][FAP] to [HMIM][FAP] whereas, the variation in this parameter is within the limits of experimental error for DMDPP.

It has been well-established[42−48] that rotational dynamics of medium sized solute molecules follows slip hydrodynamics in the absence of specific interactions. In a recent study,[14] we have examined the rotational dynamics of structurally similar R110 and 9-phenylanthracene (9-PA) in 1-butyl-3-methylimidazolium hexafluorophosphate ([BMIM][PF_6^-]) as a function of temperature. It has been observed that the rotational dynamics of R110 is close to the stick limit and the rotation of nonpolar solute 9-PA follows slip hydrodynamics. Specific interactions between the cationic solute and the hexafluorophosphate anion of the ionic liquid have been invoked to explain the observed slow rotation. Similarly, even in the present case, specific interactions between R110 and FAP anion are responsible for slower solute rotational dynamics. As mentioned in the preceding paragraph, C_{obs} values of R110 increase with an increase in the alkyl chain length of the imidazolium cation. It must, however, be noted that the extent of increase is not uniform from [EMIM][FAP] to [HMIM][FAP]. The C_{obs} for R110 increases by 27% from [EMIM][FAP] to [BMIM][FAP] and from [BMIM][FAP] to [HMIM][FAP] by a mere 4%. Somewhat similar trend has been noticed by Fruchey and Fayer[16] in a recent rotational dynamics study involving the anionic solute sodium 8-methoxypyrene-1,3,6-sulfonate (MPTS) in 1-alkyl-3-methyllimidazolium bis(trifluoromethylsulfonyl)imides. They have observed an increase of 6% and 17%, respectively, in the C_{obs} values of MPTS from ethyl to butyl and from butyl to hexyl derivatives. These results have been rationalized by invoking the "solventberg" model[49,50] wherein association of a larger solvent molecule with the rotating solute molecule increases the effective hydrodynamic volume of the solute. The same arguments can be used to account for the trends observed in the present study. However, it is rather difficult to comprehend as to why the differences in the C_{obs} values are not uniform from [EMIM][FAP] to [HMIM][FAP].

Alternatively, it has been suggested that reorientation time of a solute molecule depends on the strength of the solute−solvent hydrogen bond.[29] It must be noted that specific interactions influence molecular rotation only if hydrogen bonding dynamics takes place on a time scale that is comparable to or slower than the time scale of molecular rotation. If there is some flexibility of the hydrogen bonds to angular motion, the small-step angular displacement occurring during the lifetime of a hydrogen bond will not cause any solvent to be dragged along, thus there will be no effect on molecular rotation.[51,52] On the other hand, if the solute−solvent hydrogen bonds are strong enough, they will remain intact during the course of the rotation. In other words, stronger solute−solvent hydrogen bonds lead to slower rotation of the solute. In fact, this hypothesis has been verified in case of the rotational dynamics of DMDPP and its hydrogen bonding counterpart, 1,4-dioxo-3,6-diphenylpyrrolo[3,4-*c*]pyrrole (DPP) in ethanol and 2,2,2-trifluoroethanol (TFE) and also in isomeric butanols by correlating the measured reorientation times with the calculated solute−solvent interaction strengths.[53,54] However, in the present scenario, it is nontrivial to visualize how the presence of longer alkyl chains on the imidazolium cation influences the hydrogen bond accepting ability of the FAP anion.

It has been reported that the hydrogen bond basicity of FAP anion is lower compared to hexafluorophosphate.[26,27] In other words, hexafluorophosphate anion is a better hydrogen bond acceptor than FAP anion. To find out how the relative hydrogen bond accepting abilities of the two anions influence the rotational dynamics of R110, C_{obs} values have been compared in the two systems. The C_{obs} values of R110 in [BMIM][FAP] and [BMIM][PF_6^-] over the temperature range 298−348 K are 0.70 ± 0.05 and 0.83 ± 0.05 (data taken from ref 14), respectively. It may appear that these numbers differ by a mere 20%. However, comparison of the data at each temperature indicates that C_{obs} values in [BMIM][FAP] decrease by 18% from 298 to 348 K whereas, these numbers in [BMIM][PF_6^-] increase by 22% with an enhancement in the temperature. It is apparent that the effect of temperature on C_{obs} is quite contrasting in these two ionic liquids. Nevertheless, it is evident from this data that stronger association between R110 and hexafluorophosphate is responsible for the observed slower rotational dynamics of the solute in [BMIM][PF_6^-] compared to [BMIM][FAP]. Thus, it would be interesting to carry out a study in a series of ionic liquids with different anions and find out whether the C_{obs} values of a cationic solute can be correlated with the hydrogen bond basicities of the anions.

As mentioned earlier, the rotational dynamics of DMDPP is closer to slip hydrodynamics and the variation in the C_{obs} values from [EMIM][FAP] to [HMIM][FAP] is negligible. It has been observed that the rotational behavior of the solute DMDPP is akin to that of a nonpolar solute in a majority of the solvents.[31] Only in case of strong hydrogen bond donating solvents, such as TFE, do the two carbonyl groups of the solute form strong enough hydrogen bonds with the solvent such that its rotation is hindered.[53] Comparison of C_{obs} values of DMDPP in [EMIM][FAP] and [HEMIM][FAP] indicates that C_{obs} is larger by 30% in the hydroxyl derivative. In contrast, such a difference has not been noticed in case of R110. To further illustrate the differences in the rotational dynamics of DMDPP in [EMIM][FAP] and [HEMIM][FAP], the measured τ_r values of both R110 and DMDPP in [HEMIM][FAP] at each temperature were

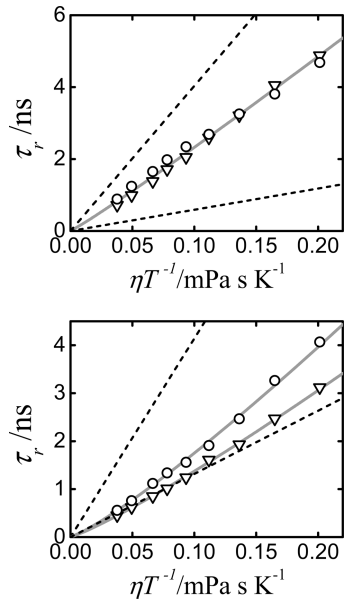

Figure 6. Comparison of the reorientation times of R110 (top) and DMDPP (bottom) in [EMIM][FAP] (▽) and [HEMIM][FAP] (○). The reorientation times in [HEMIM][FAP] were normalized to that of [EMIM][FAP] by multiplying with a normalizing factor η^* as described in the text. The lines passing through the data points are the fitted ones obtained from log−log plots of τ_r and η/T. Theoretically calculated reorientation times using SED theory with slip and stick boundary conditions are also shown (dashed lines) in the figures.

normalized with respect to the viscosity of [EMIM][FAP] by multiplying with a normalization factor η^*, which is given below.

$$\eta^* = \left(\frac{\eta_{[\mathrm{EMIM}][\mathrm{FAP}]}}{\eta_{[\mathrm{HEMIM}][\mathrm{FAP}]}}\right)_T \tag{10}$$

It may be noted that this kind of normalization is valid only when the variation of τ_r with η is linear. However, as mentioned before, the dependence of τ_r on η/T shows a slight degree of nonlinearity. Although the degree of nonlinearity for R110 and DMDPP are 1.04 and 1.15, respectively, these numbers are more or less identical for a given solute in [EMIM][FAP] and [HEMIM][FAP]. Thus, the normalization process carried out either using eq 10 or by considering the nonlinear dependence of τ_r on η/T yielded similar results. Plots of τ_r versus η/T for R110 and DMDPP in [EMIM][FAP] together with normalized reorientation times in [HEMIM][FAP] are displayed in Figure 6. In case of R110, the τ_r values in [EMIM][FAP] almost overlap with the normalized reorientation times in [HEMIM][FAP] and a common relationship was obtained between τ_r and η/T from the least-squares analysis of the log−log plots, which is described by the following expression.

R110/[EMIM] & [HEMIM][FAP]

$$\tau_r = (26.7 \pm 2.3)(\eta/T)^{1.06\pm0.03}\ (N = 18, R = 0.992)$$

In contrast, the normalized reorientation times of DMDPP are longer in [HEMIM][FAP] compared to the ones measured in [EMIM][FAP] and two separate relationships were obtained between τ_r and η/T, which are given below.

DMDPP/[EMIM][FAP]

$$\tau_r = (19.6 \pm 0.6)(\eta/T)^{1.15\pm0.01}\ (N = 9, R = 0.999)$$

DMDPP/[HEMIM][FAP]

$$\tau_r = (26.3 \pm 1.3)(\eta/T)^{1.17\pm0.02}\ (N = 9, R = 0.999)$$

The observed slower dynamics of DMDPP in [HEMIM][FAP] compared to [EMIM][FAP] can be rationalized on the basis of hydrogen bond donating ability of the hydroxyl group attached to the imidazolium cation. Using the solvation parameter model,[55] Anderson and co-workers[26] have found that the presence of FAP increases the hydrogen bond acidity of the 1-(2-hydroxyethyl)-3-methylimidazolium cation. Thus, due to the enhanced hydrogen bond donating ability of [HEMIM], strong hydrogen bonding interactions prevail between the carbonyl groups of DMDPP and the hydroxyl group of the imidazolium cation, which results in the slower rotation of the solute.

Conclusions

In an attempt to explore the role of specific interactions on the rotational dynamics of charged and neutral solutes in ionic liquids, time-resolved fluorescence anisotropy measurements of R110 and DMDPP have been carried out as a function of temperature in a series of 1-alkyl-3-methylimidazolium ionic liquids containing FAP anion. The important findings are summarized in this section. Rotational dynamics of R110 is closer to the predictions of stick hydrodynamics as a consequence of strong association between the cationic solute and the FAP anion of the ionic liquids. An increase in the alkyl chain length on the imidazolium cation has a small but discernible influence on the rotational dynamics of R110, and this observation has been rationalized using the solventberg model. According to this model, association of the solute molecule with a larger solvent molecule increases the effective hydrodynamic volume of the rotating entity, which results in the slower rotational dynamics of the solute. In contrast to the cationic solute, the rotational dynamics of the neutral solute, DMDPP follows slip hydrodynamics, which is in accord with the theoretical prediction for a medium sized solute molecule. It has been noticed that the length of the alkyl chain on the imidazolium cation has no bearing on the rotation of DMDPP. The slower rotation of DMDPP in [HEMIM][FAP] compared to that observed in [EMIM][FAP] has been rationalized on the basis of hydrogen bonding interactions between the carbonyl groups of DMDPP and the hydroxyl group of the imidazolium cation.

Acknowledgment. Mr. Chetan Shah is acknowledged for his help with the viscosity measurements. This work is supported by the financial assistance from the Department of Atomic Energy for the project No.2008/38/04-BRNS.

References and Notes

(1) Welton, T. *Chem. Rev.* **1999**, *99*, 2071.
(2) Wasserscheid, P.; Keim, W. *Angew. Chem., Int. Ed.* **2000**, *39*, 3772.
(3) Wasserscheid, P., Welton, T., Eds. *Ionic Liquids in Synthesis*; Wiley-VCH: Weinheim, Germany, 2003.
(4) Adams, D.; Dyson, P.; Tavener, S. *Chemistry in Alternative Reaction Media*; John Wiley & Sons: New York, 2004.
(5) Yao, C.; Pitner, W. R.; Anderson, J. L. *Anal. Chem.* **2009**, *81*, 5054.
(6) Baker, S. N.; Baker, G. A.; Kane, M. A.; Bright, F. V. *J. Phys. Chem. B* **2001**, *105*, 9663.
(7) Antony, J. H.; Mertens, D.; Dölle, A.; Wasserscheid, P.; Carper, W. R. *ChemPhysChem* **2003**, *4*, 588.

(8) Ingram, J. A.; Moog, R. S.; Ito, N.; Biswas, R.; Maroncelli, M. *J. Phys. Chem. B* **2003**, *107*, 5926.
(9) Ito, N.; Arzhantsev, S.; Heitz, M.; Maroncelli, M. *J. Phys. Chem. B* **2004**, *108*, 5771.
(10) Ito, N.; Arzhantsev, S.; Maroncelli, M. *Chem. Phys. Lett.* **2004**, *396*, 83.
(11) Jin, H.; Baker, G. A.; Arzhantsev, S.; Dong, J.; Maroncelli, M. *J. Phys. Chem. B* **2007**, *111*, 7291.
(12) Funston, A. M.; Fadeeva, T. A.; Wishart, J. F.; Castner, E. W. *J. Phys. Chem. B* **2007**, *111*, 4963.
(13) Mali, K. S.; Dutt, G. B.; Mukherjee, T. *J. Chem. Phys.* **2005**, *123*, 174504.
(14) Mali, K. S.; Dutt, G. B.; Mukherjee, T. *J. Chem. Phys.* **2008**, *128*, 054504.
(15) Paul, A.; Samanta, A. *J. Phys. Chem. B* **2007**, *111*, 4724.
(16) Fruchey, K.; Fayer, M. D. *J. Phys. Chem. B* **2010**, *114*, 2840.
(17) Chakrabarty, D.; Chakraborty, A.; Seth, D.; Sarkar, N. *J. Phys. Chem. A* **2005**, *109*, 1764.
(18) Sarkar, S.; Pramanik, R.; Ghatak, C.; Setua, P.; Sarkar, N. *J. Phys. Chem. B* **2010**, *114*, 2779.
(19) Ignat'ev, N. V.; Welz-Biermann, U.; Kucheryna, A.; Bissky, G.; Willner, H. *J. Fluorine Chem.* **2005**, *126*, 1150.
(20) O'Mahony, A. M.; Silvester, D. S.; Aldous, L.; Hardacre, C.; Compton, R. G. *J. Chem. Eng. Data* **2008**, *53*, 2884.
(21) Freemantle, M. *Chem. Eng. News* **2004**, *82*, 44.
(22) El Abedin, S. Z.; Borissenko, N.; Endres, F. *Electrochem. Commun.* **2004**, *6*, 422.
(23) Muldoon, M. J.; Aki, S. N. V. K.; Anderson, J. L.; Dixon, J. K.; Brennecke, J. F. *J. Phys. Chem. B* **2007**, *111*, 9001.
(24) Endres, F.; MacFarlane, D.; Abbott, A. *Electro Deposition from Ionic Liquids*; Wiley-VCH: NewYork, 2008.
(25) Dyson, P. J.; Laurenczy, G.; Ohlin, C. A.; Vallance, J.; Welton, T. *Chem. Commun.* **2003**, 2418.
(26) Zhao, Q.; Eichhorn, J.; Pitner, W. R.; Anderson, J. L. *Anal. Bioanal. Chem.* **2009**, *395*, 225.
(27) Anderson, J. L.; Ding, J.; Welton, T.; Armstrong, D. W. *J. Am. Chem. Soc.* **2002**, *124*, 14247.
(28) O'Connor, D. V.; Phillips, D. *Time-Correlated Single Photon Counting*; Academic Press: London, 1984.
(29) Fleming, G. R. *Chemical Applications of Ultrafast Spectroscopy*; Oxford University Press: New York, 1986.
(30) Waldeck, D. H. In *Conformational Analysis of Molecules in Excited States*; Waluk, J., Ed.; Wiley-VCH: New York, 2000.
(31) Dutt, G. B. *ChemPhysChem* **2005**, *6*, 413.
(32) Hu, C. M.; Zwanzig, R. *J. Chem. Phys.* **1974**, *60*, 4354.
(33) Perrin, F. *J. Phys. Radium* **1934**, *5*, 497.
(34) Dutt, G. B.; Sachdeva, A. *J. Chem. Phys.* **2003**, *118*, 8307.
(35) Edward, J. T. *J. Chem. Educ.* **1970**, *47*, 261.
(36) Small, E. W.; Isenberg, I. *Biopolymers* **1977**, *16*, 1907.
(37) Sension, R. J.; Hochstrasser, R. M. *J. Chem. Phys.* **1993**, *98*, 2490.
(38) Einstein, A. *Investigations on the Theory of Brownian Movement*; Dover: New York, 1956.
(39) Hartman, R. S.; Konitsky, W. M.; Waldeck, D. H.; Chang, Y. J.; Castner, E. W. *J. Chem. Phys.* **1997**, *106*, 7920.
(40) Dutt, G. B.; Singh, M. K.; Sapre, A. V. *J. Chem. Phys.* **1998**, *109*, 5994.
(41) Alavi, D. S.; Waldeck, D. H. *J. Phys. Chem.* **1991**, *95*, 4848.
(42) Ben-Amotz, D.; Scott, T. W. *J. Chem. Phys.* **1987**, *87*, 3739.
(43) Ben-Amotz, D.; Drake, J. M. *J. Chem. Phys.* **1988**, *89*, 1019.
(44) Kim, S. K.; Fleming, G. R. *J. Phys. Chem.* **1988**, *92*, 2168.
(45) Roy, M; Doraiswamy, S. *J. Chem. Phys.* **1993**, *98*, 3213.
(46) Anderton, R. M.; Kauffman, J. F. *J. Phys. Chem.* **1994**, *98*, 12117.
(47) De Backer, S.; Dutt, G. B.; Ameloot, M; De Schryver, F. C.; Müllen, K.; Holtrup, F. *J. Phys. Chem.* **1996**, *100*, 512.
(48) Benzler, J.; Luther, K. *Chem. Phys. Lett.* **1997**, *279*, 333.
(49) Spears, K. G.; Cramer, L. E. *Chem. Phys.* **1978**, *30*, 1.
(50) Spears, K. G.; Steinmetz, K. M. *J. Phys. Chem.* **1985**, *89*, 3623.
(51) Chuang, T. J.; Eisenthal, K. B. *Chem. Phys. Lett.* **1971**, *11*, 368.
(52) Eisenthal, K. B. *Acc. Chem. Res.* **1975**, *8*, 118.
(53) Dutt, G. B.; Ghanty, T. K. *J. Chem. Phys.* **2003**, *119*, 4768.
(54) Dutt, G. B.; Ghanty, T. K. *J. Phys. Chem. A* **2004**, *108*, 6090.
(55) Abraham, M. H. *Chem. Soc. Rev.* **1993**, *22*, 73.

JP1039282